RESEARCH ARTICLE

Efficient CRISPR/Cas9-mediated genome editing in the European corn borer, *Ostrinia nubilalis*

Jacob N. Dayton [ORCID] | Tammy T. Tran | Elisa Saint-Denis | Erik B. Dopman

Department of Biology, Tufts University, Medford, Massachusetts, USA

Correspondence
Jacob N. Dayton, Department of Biology, Tufts University, 200 Boston Avenue Suite 4700, Medford, MA, USA.
Email: jacob.dayton@tufts.edu

Abstract

The European corn borer (*Ostrinia nubilalis*) is an agricultural pest and burgeoning model for research on speciation, seasonal adaptation and insect resistance management. Although previous work in *O. nubilalis* has identified genes associated with differences in life cycle, reproduction, and resistance to *Bt* toxins, the general lack of a robust gene-editing protocol for *O. nubilalis* has been a barrier to functional validation of candidate genes. Here, we demonstrate an efficient and practical methodology for heritable gene mutagenesis in *O. nubilalis* using the CRISPR/Cas9 genome editing system. Precise loss-of-function (LOF) mutations were generated at two circadian clock genes, *period* (*per*) and *pigment-dispersing factor receptor* (*pdfr*), and a developmental gene, *prothoracicotropic hormone* (*ptth*). Precluding the need for a visible genetic marker, gene-editing efficiency remained high across different single guide RNAs (sgRNA) and germline transmission of mutations to F_1 offspring approached 100%. When single or dual sgRNAs were injected at a high concentration, gene-specific phenotypic differences in behaviour and development were identified in F_0 mutants. Specifically, F_0 gene mutants demonstrated that PER, but not PDFR, is essential for normal timing of eclosion. PTTH F_0 mutants were significantly heavier and exhibited a higher incidence of diapause. This work will accelerate future studies of gene function in *O. nubilalis* and facilitate the development of similar screens in other Lepidopteran and non-model insects.

KEYWORDS
Cas9, circadian, European corn borer, period, pigment dispersing factor receptor, prothoracicotropic hormone

INTRODUCTION

As a pest, the European corn borer (*Ostrinia nubilalis*) is responsible for substantial yield losses in corn and other crops worldwide. Although *Bacillus thuringiensis* (*Bt*) maize adoption (1996–2016) in the United States led to regional suppression of *O. nubilalis* (Dively et al., 2018), the first case of practical resistance to *Bt* Cry1F maize was identified in Nova Scotia, Canada, in 2018 (Smith et al., 2019). Since then, resistance to *Bt* Cry proteins has been documented in other regions of Canada and observed on a sweet corn plot producing Cry1A.105 and Cry2Ab2 proteins in Connecticut, USA (NC 246, 2024). Although gene regions segregating with resistance

have been identified (Coates et al., 2011; Coates & Siegfried, 2015; Farhan et al., 2023), functional validation by gene knockout is needed to enhance sequence-based resistance monitoring (Pezzini et al., 2024) and provide mechanistic insight into cross-resistance between pyramided *Bt* toxins and foliar sprays (Abdelgaffar et al., 2021).

Beyond *Bt* resistance, prior quantitative trait locus mapping and genomic approaches have identified candidate genes associated with other traits of agroeconomic importance. For example, population differences in *O. nubilalis* female pheromone composition (Dopman et al., 2004; Lassance et al., 2010) and male preference (Unbehend et al., 2021) could alter the efficacy of passive monitoring techniques

(i.e., pheromone lures) and affect the rate at which resistance alleles evolve by gene flow. Additionally, life cycle differences in generation number (voltinism; Kozak et al., 2019; Levy et al., 2015) determine the distribution and abundance of pests across space, time and host plants. Consequently, there is a need for robust genetic techniques to probe the genetic basis of these pest traits. Considering that the function (Mackay & Anholt, 2024) and evolution (Dopman et al., 2024; Tigano & Friesen, 2016) of a gene depends on its genetic background, greater understanding of the genetic mechanisms underlying behavioural and ecological differences among corn borer populations is critical to effective integrated pest management and insect resistance management for this insect (Coates et al., 2018).

The advent of CRISPR/Cas9 genome editing has revolutionized the study of gene function in insects (Taning et al., 2017). This system utilizes a single guide RNA (sgRNA) to direct the Cas9 nuclease to specific, complementary genomic loci, where it induces a double-strand break (DSB) upstream of the protospacer adjacent motif (PAM). Aberrant repair of these breaks allows for targeted disruption, insertion, or replacement of genes (Taning et al., 2017). Particularly in *O. nubilalis* and other Lepidoptera, where conventional methods like RNA interference (RNAi) are inefficient and often falter (Cooper et al., 2021; Guan et al., 2018; Khajuria et al., 2011; Terenius et al., 2011), CRISPR/Cas9 has paved the way for numerous studies of gene function. These endeavours have illuminated key mechanisms underlying diverse phenotypic traits, ranging from pigmentation and wing patterning to development and reproductive behaviour (Li et al., 2021).

In this study, we demonstrate that CRISPR/Cas9 is a highly efficient and robust tool for generating heritable mutations in *O. nubilalis*. We used both single and dual sgRNAs to generate LOF mutants for three genes. Across targets, editing efficiency remained high and sufficient for streamlined studies of gene function in F_0 mutants. We also describe an approach for quantifying interactions between mutations and their genetic background. This methodology should accelerate future genetic studies in *O. nubilalis* and facilitate similar screens in other related insects.

RESULTS AND DISCUSSION

Efficient CRISPR/Cas9-mediated mutagenesis

To assess the capacity for CRISPR/Cas9-mediated genome-editing to produce LOF mutations in *O. nubilalis*, we targeted two circadian clock genes, *period* (Konopka & Benzer, 1971) and *pigment dispersing factor receptor-like* (*pdfr*; Hyun et al., 2005; Lear et al., 2005; Mertens et al., 2005). PERIOD is involved in the main transcriptional repression by CRYPTOCHROME 2 of the Lepidopteran circadian clock (reviewed in Brady et al., 2021), oscillating in abundance every ∼24 h in both entrained (light:dark, LD) and free-running (continuous darkness, DD) conditions (Hardin et al., 1990, 1992). Meanwhile, *pdfr* encodes the extracellular receptor for the neuropeptide pigment dispersing factor (PDF, Renn et al., 1999). PDF/PDFR signalling synchronizes transcriptional oscillations between clock neurons, helping maintain robust

behavioural rhythms in DD (Lin et al., 2004; Peng et al., 2003; Renn et al., 1999) and adjusting these rhythms to seasonal changes in LD cycles (Ruf et al., 2021; Yoshii et al., 2009). In addition to their roles in the circadian clock network, in *O. nubilalis*, genetic differences at Z-linked *period* and *pdfr* are associated with the 14–21 day delay in spring emergence that contributes to the life cycle difference in the number of generations per growing season between univoltine (*period^{U}pdfr^U*) and bivoltine (*period^{B}pdfr^B*) populations (Kozak et al., 2019). Univoltine prepupae also exhibit a relative increase in their propensity for seasonal diapause (Ikten et al., 2011; Yu, 2022) and an earlier peak adult activity under DD (Dayton & Owens, 2024; Kozak et al., 2019).

For the CRISPR/Cas9 system, gene-specific sgRNAs were designed on the *O.nubilalis* RefSeq assembly (GCF_963855985.1) to target the coding sequences of *period* (GenBank: LOC135086880) and *pdf receptor-like* (GenBank: LOC135087024; Figure 1, Table S1). Following oviposition by univoltine (*period^{U}pdfr^U*)and bivoltine (*period^{B}pdfr^B*) females, clusters of embryos were injected with Cas9:sgRNA ribonucleoprotein (RNP) complexes in 2022 (2.5 μM Cas9, 150 ng/μL sgRNA). To test the effects of different sgRNA concentrations on somatic editing efficiency, eggs were injected with a higher sgRNA concentration in 2023 (2.5 μM Cas9, 180 ng/μL sgRNA). Typically, 7–12 embryos were injected per cluster. After hatching, injected F_0 was tracked throughout development. Most injected F_0 individuals that hatched survived to adulthood (Table 1), with an average of six F_0 per injected cluster (95% confidence interval [CI]: 3.5–9.0). Mating success did not differ significantly across sgRNAs (binomial GLM; LR $\chi^2 = 2.83$, df $= 2$, $p = 0.243$) or injection year ($\chi^2 = 0.50$, df $= 1$, $p = 0.481$; Table 1). After mating, successful F_0 parents were screened for CRISPR/Cas9-induced mutations by polymerase chain reaction (PCR) and Sanger sequencing. Individuals were classified as somatic mutants if they exhibited >20% indel frequency, as estimated by deconvolution of Sanger sequence electropherograms (DeLay et al., 2018; Synthego Performance Analysis, 2019).

CRISPR/Cas9 was highly effective. Across years and loci, 74% (95% CI: 60%–89%) of F_0 individuals were somatic mutants. Somatic editing efficiency was robust to the sgRNA (binomial GLM; LR $\chi^2 = 1.02$, df $= 2$, $p = 0.601$) and injection year (LR $\chi^2 = 2.57$, df $= 1$, $p = 0.11$; Table 1), and the overall efficiency was comparable to or higher than reports from other Lepidoptera (see Supporting Results in Supporting Information S1). In fact, editing efficiency was so high that nearly 100% of mutations in the F_0 were heritable and transmitted to F_1 progeny (Table 1). Although the classification as 'somatic mutant' is binary, the F_0 injected in 2023 (86% indels) exhibited significantly greater conversion of wildtype alleles than the F_0 from 2022 (78% indels; Wilcoxon Sign-Ranked W $= 143$, $p = 0.049$), underscoring a possible impact of the increase in sgRNA concentration (1.2-fold) on editing efficiency (Bassett et al., 2013; Perera et al., 2018; Wang et al., 2013).

Diverse mutations were observed at *period* (Figure 1a) and *pdfr* (Figure 1b). Deletions were more frequent than insertions ($\chi^2 = 14.52$, df $= 1$, $p < 0.001$) and represented 82% (95% CI: 37%–100%) of all sequenced mutations. 78% (95% CI: 64%–92%) of mutations were frameshifts that produced a premature stop codon,
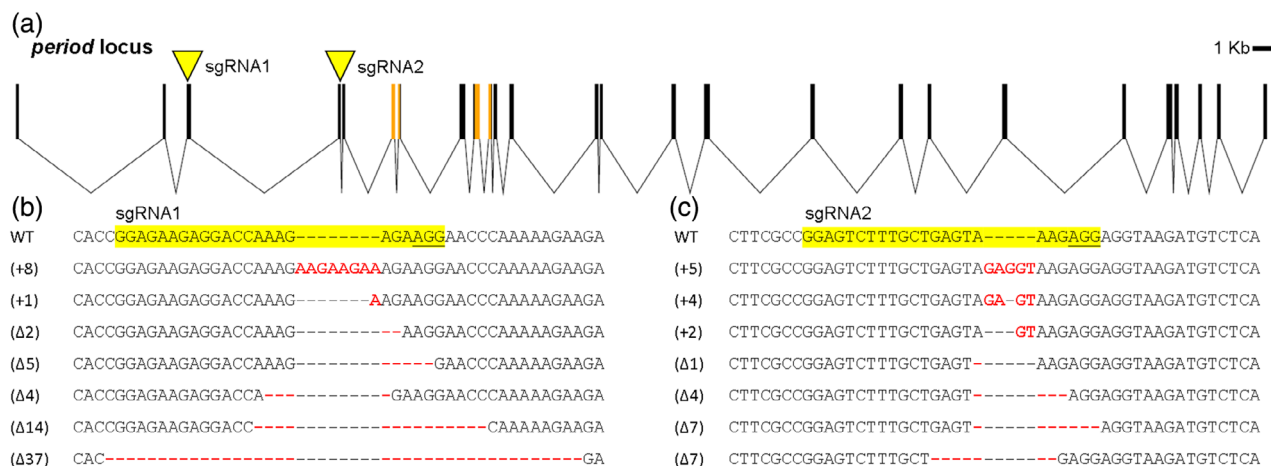
FIGURE 1 CRISPR/Cas9-mediated mutagenesis of *O. nubilalis* genes *period* and *pdfr*. (a) (Top) Exon-intron gene model of the *period* coding sequence (exons 2–27; GenBank: LOC135086880). Yellow triangles indicate approximate positions of sgRNA recognition sequences in exon 4 and exon 5. Predicted PAS domains are coloured orange. (Bottom) Representative frameshift mutations induced by microinjection of single sgRNA1:Cas9 and sgRNA2:Cas9 mixtures. The protospacer adjacent motif (PAM site, 5′-NGG-3′) within the highlighted sgRNA target sequence is underlined. Compared to the wildtype (WT) sequence, red dashes and bases denote deletions and insertions, respectively. (b) (Top) Exon-intron gene model of the *pdf receptor-like* (*pdfr*) coding sequence (exons 2–11; GenBank: LOC135087024). Yellow triangles indicate the sgRNA recognition sequences in exon 7 and the predicted C-terminal domain is in orange. (Bottom) Representative induced mutations annotated as in (a).

TABLE 1 CRISPR/Cas9-induced mutagenesis in *O. nubilalis*. Single Cas9:sgRNA mixtures targeting the *period* and *pigment-dispersing factor receptor-like* (*pdfr*) genes were microinjected into *O. nubilalis* eggs.

	Target (sgRNA)	Injected clusters	Survived to adult, N (%)	% successful matings (n)	% somatic F_0 mutants (n)	% germline F_1 mutation rate (n)
2022	*period* (1)	12	67 (81%)	49% (51)	58% (19)	86% (7)
	period (2)	12	50 (65%)	48% (42)	80% (15)	100% (4)
	pdfr (1)	4	11 (52%)	78% (9)	71% (7)	100% (3)
2023	*period* (1)	8	56 (nd)	63% (27)	93% (15)	100% (5)
	period (2)	8	79 (nd)	51% (43)	84% (19)	100% (5)
	pdfr (1)	4	33 (nd)	64% (14)	60% (5)	100% (2)
			Grand mean	58% (47–71%)	74% (60–89%)	98% (92–100%)

Note: Percent survival was not determined (nd) in 2023. The percentage of successful matings was determined from a subset (n) of the total individuals that survived to adulthood. Similarly, the percentage of somatic mutants is based on the number of genotyped (n) fertile F_0 adults that presented somatic mosaicism >20%. Germline mutation rate corresponds to the percentage of F_1 progeny with a mutated allele of the total progeny genotyped (n). Grand means with 95% confidence interval are provided in the bottom row.

significantly more than expected for indels within a coding sequence (i.e., two out of every three; $\chi^2 = 4.08$, df = 1, $p = 0.043$; Wu et al., 2018). These frameshift mutations were considered LOF null alleles, as they were predicted to encode extensively truncated proteins of PERIOD (wildtype: 1159 amino acids vs. sgRNA1: 67–89 amino acids, sgRNA2: 139–152 amino acids) and PDFR (wildtype: 431 amino acids; sgRNA1: 224 amino acids).

Mutagenesis of *period* but not *pdfr* disrupts rhythmic eclosion

To assess the phenotypic effect of *period* and *pdfr* on circadian behaviour in the corn borer, we examined the timing that adult moths eclosed from their pupal case under a summer-like photoperiod (LD 16:8 h; e.g., Markert et al., 2016). Eclosion was described in Arbitrary Zeitgeber Time (AZT) when AZT0 was the time that lights turned on. The rhythmic strength of eclosion timing was quantified by the proportion of moths who eclosed within a peak 8-h eclosion window/ gate (e.g., Ikeda et al., 2021; Liu et al., 2023; Winfree, 1970). Genetic background (univoltine/bivoltine) of wildtype and mutants did not influence rhythmic strength (binomial GLM; $\chi^2 = 0.08$, df = 1, $p = 0.78$; AIC = 64.5; Figure S1), so strains were combined for subsequent analyses (Figure 2; AIC = 59.0). Most wildtype adults eclosed within an 8-h gate from AZT15 to AZT22 in 2022 (0.83, 95% CI: 0.77–0.89) and in 2023 (0.75, 95% CI: 0.70–0.80; Figure 2, Figure S2).

Eclosion within this gate was significantly affected by mutagenesis of *per/pdfr* (binomial GLM; LR $\chi^2 = 40.9$, df = 2, $p < 1 \times 10^{-9}$) and
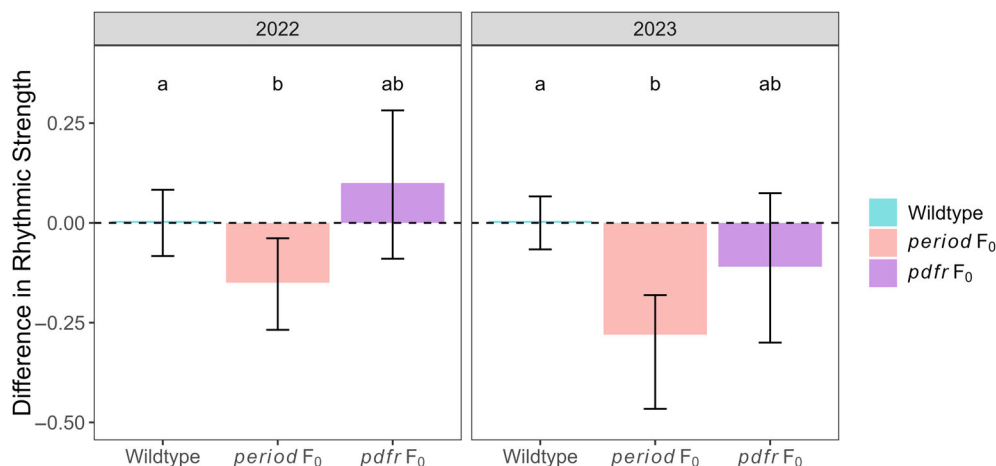
FIGURE 2 *period* but not *pdfr* mutagenesis reduces rhythmic strength in wildtype eclosion timing. Wildtype *Ostrinia nubilalis* were injected with Cas9:sgRNA targeting *period* and *pdfr* in 2022 and 2023. Eclosion of uninjected wildtype and injected F_0 adults exposed to 16L:8D hour were monitored in Arbitrary Zeitgeber Time (AZT). Rhythmic strength was quantified as the proportion of adults that eclosed from their pupal case between AZT15 and AZT22, the 8 h window encapsulating the time most wildtype adults emerge. The main effects of treatment and injection year on the rhythmic strength were modelled by a binomial logistic regression (AIC = 59.0, df = 5). Within each year, the difference in rhythmic strength (a proportion) between wildtype and the *period* versus *pdfr* F_0 was determined. Significant differences between groups were measured by Wald's test and do not encompass zero (i.e., no difference). Letters denote significant differences among groups ($p < 0.05$), with B-Y adjustment for multiple comparisons. Error bars represent 95% confidence intervals.

injection year (LR $\chi^2 = 17.4$, df = 1, $p < 3 \times 10^{-5}$), with little evidence of an interaction ($F = 2.87$, df = 2, $p = 0.238$). Specifically, mutagenesis of *period* significantly decreased rhythmic strength/gating of eclosion in 2022 (difference = −0.15, 95% CI: −0.27 to −0.04; $p = 0.006$) and 2023 (−0.28, 95% CI: −0.47 to −0.18; $p = 1 \times 10^{-8}$; Figure 2). The more pronounced phenotypic effect of *period* mutation in 2023 was consistent with the higher concentration of sgRNAs and greater observed conversion of wildtype to null alleles (see above). This reduction in rhythmic strength was concordant with significantly different distribution of eclosion across the entire 24-h distribution (Figures S1 and S2). Overall, the aberrant gating and distribution of eclosion observed for our *period* F_0 mutants recapitulated phenotypes of stable germline clock mutants in other insects. For instance, in *Drosophila melanogaster*, rhythmic strength in *period* knockouts was reduced in LD and, in the absence of light entrainment, was entirely disrupted in DD (Konopka & Benzer, 1971; Qiu & Hardin, 1996; Ruf et al., 2021). In Lepidoptera, clock gene mutation similarly reduced eclosion rhythms in LD and completely abolished them in DD (*Bombyx mori*: Ikeda et al., 2021, Nartey et al., 2021; *Helicoverpa armigera*: Liu et al., 2023). Although expression of target clock genes was not measured in our study, aberrant behavioural rhythms in eclosion have been linked to disrupted molecular rhythms in circadian transcription in the brain (Ikeda et al., 2021; Markert et al., 2016; Nartey et al., 2021). Together, our mutants provide one more layer of genetic evidence highlighting the conserved essentiality of the circadian clock for the normal timing of insect eclosion (Truman & Riddiford, 1974).

Unlike *period*, mutations in *pdfr* did not alter the rhythmic strength of eclosion in 2022 (0.10, 95% CI: −0.09 to 0.28; $p = 0.575$) or 2023 (−0.11, 95% CI: −0.30 to 0.07; $p = 0.230$; Figure 2). These observations were similar to those in *D. melanogaster*, wherein

persistent coupling of pacemaker neurons by short LD cycles (Vaze & Helfrich-Förster, 2021; Yoshii et al., 2009) masks the effects of *pdf/pdfr* loss and behavioural rhythms remain largely unaffected (Hyun et al., 2005; Myers et al., 2003; Renn et al., 1999; Ruf et al., 2021). Instead, the consequences of *pdf/pdfr* mutations in *Drosophila* are apparent in DD, when transcription oscillations among pacemaker neurons become desynchronized (Lin et al., 2004; Peng et al., 2003; Renn et al., 1999) and output behavioural rhythms rapidly dampen (Hyun et al., 2005; Myers et al., 2003; Renn et al., 1999; Ruf et al., 2021). Additionally, *pdf/pdfr* mutants in *Drosophila* are unable to entrain and adjust their locomotor activity to longer photoperiods (Vaze & Helfrich-Förster, 2021; Yoshii et al., 2009). Future studies on F_1 mutants in *O. nubilalis* will need to investigate the effects of *pdfr* loss on behavioural rhythms in DD and multiple LD photoperiods.

Targeted deletion of prothoracicotropic hormone by dual sgRNA injections

We expanded our investigation on the utility of CRISPR/Cas9 by simultaneously injecting multiple sgRNAs that targeted different regions of the *prothoracicotropic hormone* (*ptth*) gene. While the use of a single sgRNA successfully generated small indels at *period* and *pdfr* (Table 1 and Figure 1), we predicted that co-injecting two co-directional sgRNAs could induce large-scale LOF mutations, increase the frequency of null allele conversion within an individual (Kroll et al., 2021), and facilitate more rapid screening by PCR-based fragment size differences (e.g., Han et al., 2024; Markert et al., 2016; Zhao et al., 2023). Two co-directional sgRNAs were designed to target the 5′UTR and coding exon 1 of *ptth* (GenBank: LOC135088612;
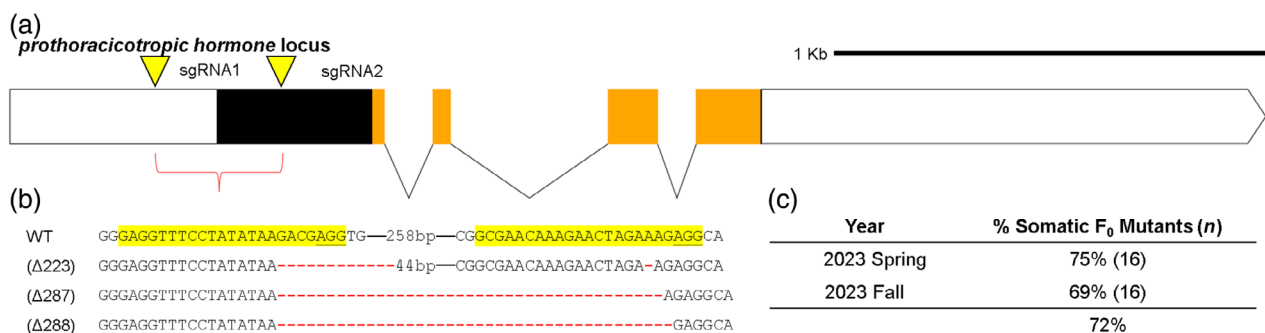
FIGURE 3 Efficient deletion of *prothoracicotropic hormone* by dual sgRNAs. (a) (Top) Exon-intron gene model of *prothoracicotropic hormone* (*ptth*) (GenBank: LOC135088612). Yellow triangles indicate the sgRNA recognition sequences in the 5'-UTR and exon 1 and the red bracket denotes the predicted interior deletion (Δ285 bp). The exons corresponding to the predicted bioactive PTTH peptide are in orange. (b) (Bottom) Representative frameshift mutations induced by microinjection of dual sgRNA1 + sgRNA2:Cas9. The protospacer adjacent motif (PAM site, 5'-NGG-3') of the highlighted sgRNA target sequences are underlined. Red dashes denote deletions compared to the wildtype (WT) reference. (c) The percentage of somatic mutants is based on the number (*n*) of genotyped F_0 individuals that presented somatic mosaicism >20%.

Figure 3), immediately upstream of the region encoding the cleaved bioactive PTTH peptide (reviewed in W. Smith & Rybczynski, 2012).

Cas9:dual sgRNA complexes were injected into early-stage embryos and a random sample of larvae and adults were screened for mutations (2.5 μM Cas9, 180 ng/μL sgRNA). Consistent with the *period* and *pdfr* injections, 72% of F_0 were somatic mutants (95% CI: 56%–88%, *n* = 32), and 59% (95% CI: 36%–77%, *n* = 23) of these mutants bore large deletions (>200 bp; Figure 3). These deletions eliminated the original *ptth* start codon and were expected to be LOF alleles (0–24 amino acids) for PTTH (221 amino acids). Notably, three F_0 mutants from spring and fall 2023 possessed a 1 bp frameshift deletion located 200 bp downstream of the sgRNA2 PAM sequence (117 amino acids) and did not present any mutations in either sgRNA recognition sequence. Considering that homology-directed repair of DSBs is dependent upon error-prone DNA polymerases, these distal frameshift mutations could be signatures of the hypermutation tracts known to extend from a DSB site (Deem et al., 2011; reviewed in Nambiar et al., 2022). Like *period* and *pdfr* injections in 2023, the high efficiency and LOF mutations demonstrated in *ptth* suggested that phenotypes could be directly screened in *ptth* F_0.

ptth loss alters development in *O. nubilalis*

In insects, binding of the neuropeptide PTTH to its receptor on the prothoracic gland, TORSO (Rewitz et al., 2009), activates MAPK/ERK signalling and promotes synthesis of ecdysone, the developmental hormone essential for moulting and metamorphosis (reviewed in W. Smith & Rybczynski, 2012). A seasonally regulated shutdown in ecdysone synthesis, attributed to the absence of PTTH secretion from the brain, is broadly considered to be the neuroendocrine basis for prepupal and pupal diapause (Denlinger et al., 2012). Furthermore, considering that both secretion of PTTH is governed by a photosensitive circadian clock (e.g., Sakurai, 1983; Selcho et al., 2017; Truman, 1972) and a functioning circadian clock is essential for seasonal responsiveness (Liu et al., 2023), it is predicted that these two

pathways converge to regulate diapause. However, the nature of this relationship between the circadian clock network, PTTH and diapause incidence has never explicitly been validated by gene knockout.

Often, the phenotypic effect(s) of mutations at a given locus depend on their genetic background. Whereby, a general framework to identify gene interactions is to screen paired wildtype versus mutant individuals across multiple backgrounds (Figure 4; Mackay & Anholt, 2024; Turner, 2014). To measure interactions between the circadian clock and *ptth*, we explored how functionally defined circadian clock alleles in bivoltine and univoltine genetic backgrounds, specifically on the Z chromosome (i.e., *period* & *pdfr*; Kozak et al., 2019; Yu, 2022), might interact with mutant *ptth* to alter development (Figure 5). For example, reciprocal crosses between each *period* background generate two sets of F_0 offspring that differ based on whether daughters inherited a bivoltine (Z^B) or univoltine (Z^U) Z chromosome from their father (note: sons are all heterozygous for Z^B/Z^U; Figure 5, *x*-axis). Since only F_0 females will differ by their genotype (e.g., Z^U/W or Z^B/W), the two populations will exhibit divergent allele frequencies on the Z chromosome (i.e., $Z^U \sim 0.75$ vs. 0.25, $Z^B \sim 0.25$ vs. 0.75; Figure 5). We injected early-stage embryos from these two populations with either Cas9:dual sgRNAs (RNPs) targeting *ptth* (see Figure 3) or a controlCas9:sgRNA mixture, to respectively generate *ptth* mutant and wildtype individuals. All individuals were phenotyped for diapause response under an inducing photoperiod (LD 15:9 h at 23.5°C); larvae were weighed on day 30 and phenotyped for diapause entry on day 38. Males and females were analysed together because there are no distinguishing morphological features present in the prepupae. A significant interaction between sgRNA treatment and candidate locus genotype on either phenotype would be consistent with strong evidence of a genetic interaction (Figure 4b; Mackay & Anholt, 2024).

However, there was no significant evidence of an interaction between *ptth* mutation and the genetic background of the Z chromosome (*period*, *pdfr*) on either mass (two-way analysis of variance: $F = 1.46$, $p = 0.229$; Figure 5a) or diapause incidence (LR $\chi^2 = 1.40$, df = 1, $p = 0.237$; Figure 5b). Instead, mass was significantly affected

(a)

Autosomal Candidate Locus *A*

Crosses:	$A_1A_2 \times A_1A_1$	$A_1A_2 \times A_2A_2$	
Offspring:	$A_1A_2 + A_1A_1$	$A_1A_2 + A_2A_2$	**Wildtype *B* (Control sgRNA)**
	$A_1A_2 + A_1A_1$	$A_1A_2 + A_2A_2$	**Mutant *B* (Target sgRNA)**

Sex-linked Candidate Locus *A*

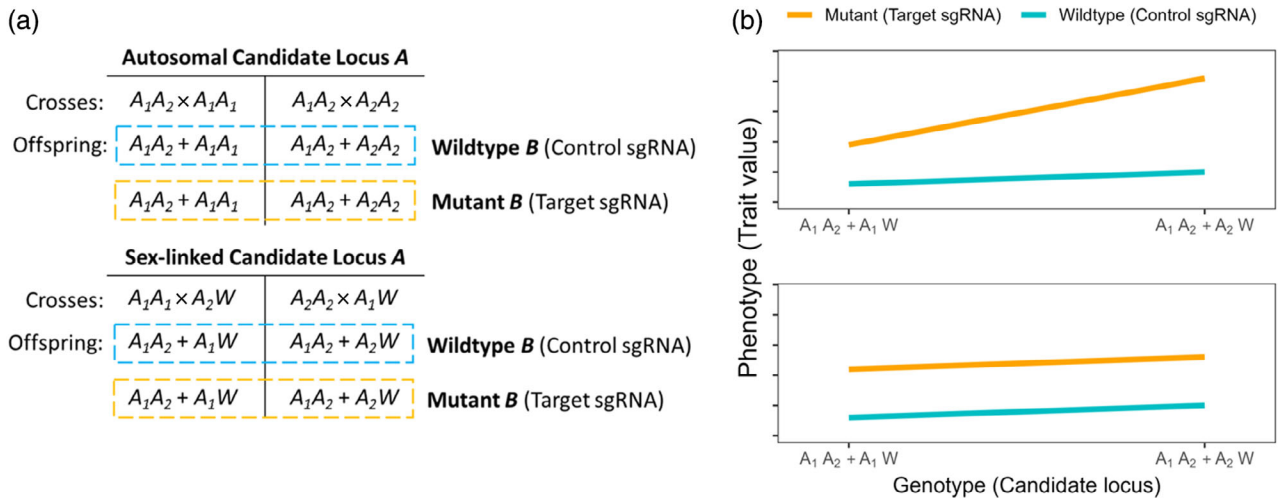| Crosses:	$A_1A_1 \times A_2W$	$A_2A_2 \times A_1W$	
Offspring:	$A_1A_2 + A_1W$	$A_1A_2 + A_2W$	**Wildtype *B* (Control sgRNA)**
	$A_1A_2 + A_1W$	$A_1A_2 + A_2W$	**Mutant *B* (Target sgRNA)**

(b)

FIGURE 4 Test for two-locus epistasis between *A* and *B* for a quantitative trait. (a) Interactions between alleles at candidate locus *A* and target locus *B* are measured in F_0 offspring derived from reciprocal crosses. Given a similar number of offspring from each genotype, all polymorphic alleles among F_0 have frequencies of 0.50, except for locus *A* (e.g., $A_2 \sim 0.25$ vs. $A_2 \sim 0.75$). To generate wildtype *B* (control) or loss-of-function (LOF) *B* mutants (sgRNA), early-stage F_0 embryos are respectively injected with a control Cas9:sgRNA or a functional Cas9:sgRNA mixture. (b) The phenotype of the quantitative trait is plotted against two paired populations with different genotypes at the *A* locus, and separately for wildtype *B* (blue) and mutant *B* (orange). Epistasis between loci is estimated by fitting a statistical model that includes the main effects of genotype for candidate locus *A* (A_1 or A_2), LOF mutations at *B* and their interaction. (b) (Top) A statistically significant interaction provides strong evidence for epistasis, in which the additive effect of locus *B* is greater in individuals from the A_2W background. (b) (Bottom) Significant main effects of *A* genotype and *B* mutation with no interaction reveal separate additive contributions of locus *A* and *B*, with no epistasis.
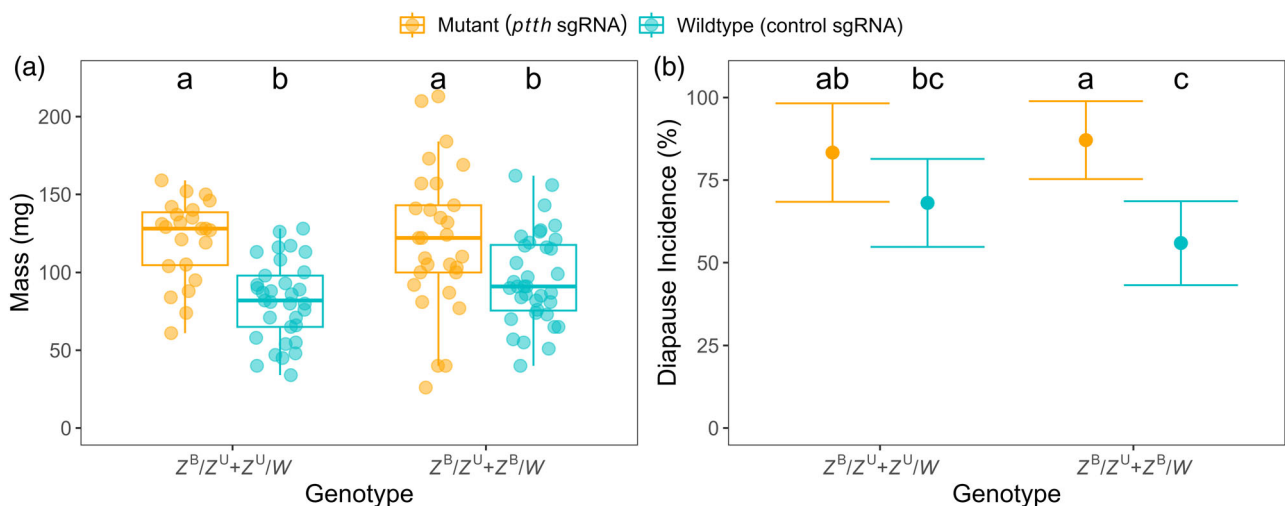

FIGURE 5 Test for two-locus epistasis between *ptth* mutants from univoltine and bivoltine backgrounds. (a) Reciprocal crosses between univoltine (Z^U) and bivoltine (Z^B) individuals generated two F_0 populations. With a similar number of male and female offspring, each F_0 population should exhibit a different allele frequency at *Z*-linked genes ($Z^U \sim 0.75$ vs. 0.25 and $Z^B \sim 0.25$ vs. 0.75; see Figure 4a). Early-stage F_0 embryos were injected with functional Cas9:sgRNA targeting *prothoracicotropic hormone* (*ptth*) or control Cas9:sgRNA to respectively generate loss-of-function (LOF) mutant *ptth* or wildtype *ptth* individuals. Following injection, F_0 was raised in 15 L:9 D hour and phenotyped for (a) body mass (day 30) and (b) diapause incidence (day 38). The phenotype of the quantitative trait is plotted against two population backgrounds for the *Z* chromosome, and separately for wildtype (blue) and mutant *ptth* (orange). Epistasis was estimated by fitting a model with main effects of *Z* background, *ptth* mutation, and their interaction on mass (normal distribution) or diapause incidence (binomial distribution). Differences between groups were measured by (a) Welch's *t*-test and (b) Wald's test. Letters denote significant differences among groups ($p < 0.05$), with a B-Y adjustment for multiple comparisons. Bars in panel (b) denote 95% confidence intervals.

by *ptth* mutation (two-way ANOVA: $F = 27.66$, $p < 1 \times 10^{-5}$) and mutants (121 mg, 95% CI: 112–130 mg) were 36% heavier than wild-type larvae (89 mg, 95% CI: 81–96 mg; Figure 5a). Genetic ablation of

PTTH signalling similarly increased body size and prolonged the larval growth period in *B. mori* (Uchibori-Asano et al., 2017; Zhang et al., 2021) and *D. melanogaster* (McBrayer et al., 2007; Rewitz

et al., 2009; Shimell et al., 2018). These conserved responses to PTTH loss were consistent with low ecdysteroid titers and past work demonstrating that low ecdysteroidogenesis by the prothoracic gland delays developmental timing and induces overgrowth (Colombani et al., 2005). Although ecdysone itself was not measured here, a reduced ecdysone titre in *ptth* F_0 mutants would be in line with the significant effect of *ptth* mutation on diapause incidence (binomial GLM; LR $\chi^2 = 10.4$, df $= 1$, $p = 0.001$; Figure 5b). Whereby, the incidence of prepupal diapause by *ptth* mutants was 24% (95% CI: 11%–37%) higher than wildtype individuals (Wald's $Z = 3.60$, $p < 0.001$; Figure 5b).

The significant additive effects of *ptth* mutation support the classic model that seasonal inhibition of PTTH secretion contributes to prepupal diapause induction (Denlinger et al., 2012). The lack of apparent epistasis between *ptth* and *period* could suggest that PTTH operates independently of or downstream of the circadian clock's role in diapause induction. However, considering that we were unable to detect known background-specific differences in diapause incidence between paired wildtype populations (Figure 5b), our study may have been underpowered and benefitted from multiple replicate populations. Additionally, genotyping to remove the genetically invariant (Z^B/Z^U) male offspring from each population would have increased the magnitude of any effect by making *Z* chromosome allele frequencies in each F_0 population (*x*-axis, Figure 5) fixed from each other.

CONCLUSIONS

We have demonstrated that the CRISPR/Cas9 system is a highly efficient and robust tool for generating LOF mutants in *O. nubilalis*. In the absence of visible markers or transposition reagents, we were able to generate precise mutations in three genes, recover a variety of mutant alleles, and capture phenotypic differences among F_0 mutants.

From start to finish, F_1-bearing germline mutations at a gene-of-interest can be isolated in one generation (35 days). When establishing stable mutant *O. nubilalis* lines, we recommend that researchers plan to outcross and screen three (95% CI: 2–5) injected F_0 adults per desired LOF mutant (Table 1 and Figure 3c). This recommended number of injected F_0 adults ($n_{\text{Injected Adults}}$) to screen per desired LOF mutant (n_{LOF}) is based on the observed (Table 1) proportion of injected adults that mated (p_{mated}), bore somatic mutations (p_{somatic}) that were frameshifts ($p_{\text{frameshift}}$), and were transmitted to F_1 offspring (n_{germline}):

$$n_{\text{Injected Adults}} = \frac{n_{\text{LOF}}}{p_{\text{germline}} \times p_{\text{frameshift}} \times p_{\text{somatic}} \times p_{\text{mating}}}$$
$$= \frac{n_{\text{LOF}}}{0.98 \times 0.78 \times 0.74 \times 0.58}$$

Depending on the lethality of the target gene and number of surviving injected adults per egg cluster, at least 0.5–1.5 egg clusters should be injected per desired LOF mutant.

Alternatively, for streamlined studies of gene function, CRISPR/Cas9 is efficient enough for immediate developmental and behavioural phenotyping of F_0 knockouts (Figures 2 and 5). To support these screens and increase the conversion of wildtype to null LOF alleles in F_0, two to three sgRNAs can be designed per coding sequence (e.g., Kroll et al., 2021; Zhu et al., 2020). See Kroll et al. (2021) for additional considerations when designing F_0 knockout screens.

Finally, although we did not identify significant evidence of two-locus epistasis, an approach that screens paired wildtype/mutant F_0 for quantitative traits from multiple backgrounds merits further exploration (Figure 4; Mackay & Anholt, 2024; Turner, 2014). Whereas this design has traditionally been limited to model organisms (e.g., *S. cerevisiae*, *C. elegans*, *D. melanogaster*), pairing modern gene-editing systems (e.g., CRISPR/Cas9) with the natural variation observed in non-model insects could revolutionize the study of genes and their modifiers on quantitative traits of agroeconomic and evolutionary interest (e.g., resistance, diapause, sexual communication).

EXPERIMENTAL PROCEDURES

Insect stocks

European corn borer (*O. nubilalis*) eggs were collected from laboratory populations maintained at Tufts University (Medford, MA). These were originally derived from populations in northeastern USA, exhibit divergent allele frequencies at *period* and *pdfr*, and have repeatedly been selected and studied for different univoltine (*period*^{U}*pdfr*^{U}) versus bivoltine (*period*^{B} *pdfr*^{B}) phenotypes (e.g., Dayton & Owens, 2024; Kozak et al., 2019). Adults were mated in cages containing ad libitum water and covered with parchment paper for oviposition. Egg clusters were cut out, suspended over artificial corn borer diet (Southland Products, USA), and reared under LD 16:8 h in a climate-controlled room (25.5°C, 50% RH).

sgRNA design and synthesis

CRISPR/Cas9 was leveraged to knockout *O. nubilalis* genes *period* (GenBank: LOC135086880), *pigment dispersing factor receptor-like* (*pdfr*, GenBank: LOC135087024) and *prothoracicotropic hormone* (*ptth*, GenBank: LOC135088612). Unique sgRNA targets were identified with the 'GN$_{19}$NGG' guide sequence in Geneious Prime 2023.0.4. (https://www.geneious.com) and scored for predicted off-targets in the *O. nubilalis* reference genome (GenBank: GCA_008921685.1). Target-specific DNA oligos were designed to be compatible with the EnGen™ sgRNA Synthesis Kit, *S. pyogenes* (New England BioLab). Oligos were synthesized by Integrated DNA Technologies and Eton Bioscience. These sequences are provided in Table S1.

Functional sgRNAs were synthesized following manufacturer's protocols, except fresh DTT aliquots were used and transcription was extended to 90 min at 37°C. sgRNAs were purified using the Monarch RNA Cleanup Kit (10 μg, New England BioLabs) and eluted in 12 μL

nuclease-free water. sgRNAs were diluted to 600 ng/μL and stored at −80°C. To form sgRNA:Cas9 (RNP) complexes, sgRNA aliquots were incubated at 70°C for 2 min and mixed with 2.5 μM EnGen® Spy Cas9 NLS (New England BioLabs) in injection buffer (5 mM KCl, 0.1 mM sodium phosphate buffer, pH 6.8). sgRNAs were mixed to a final concentration of 150 ng/μL in 2022 and 180 ng/μL in 2023. The components of the control *ptth* sgRNA mixture were the same, except the *ptth* target sgRNAs were incubated at 70°C for 8 min.

Embryo microinjection

Borosilicate glass capillaries (World Precision Instruments, #1B100-4; 1 mm outer dia., 0.58 mm inner dia.) were pulled on a Narishige PN-31 (Narishige Group) in 2022 ($Mag_{Main} = 96$, $Mag_{Sub} = 33$, Heat = 83) and 2023 ($Mag_{Main} = 58$, $Mag_{Sub} = 32.8$, Heat = 100.7). Needle tips were broken by scraping across forceps and retained if they exhibited a 30–55 kPa bubble pressure in water. Injections were made using a Mk1 micromanipulator (Singer Instruments) with a PLI-90 Pico-Injector Micromanipulator System (Harvard Apparatus): $P_{Inj} = 30–55$ kPa, $P_{Bal} = 4–6$ kPa, time = 12–22 ms. Settings were adjusted within each range to inject approximately 1–3 nL RNP solution per egg, as estimated by 0.01 mm calibration slide (Amscope, MR095).

Peak oviposition of *O. nubilalis* exposed to LD 16:8 h occurs within the first 2 h of darkness. Following the onset of oviposition, parchment paper containing *O. nubilalis* egg clusters (embryos) was collected every 25 min. The paper was cut into strips with individual egg clusters, and these were taped onto the lid of a plastic cell culture dish (Figure S3). Under a dissecting microscope, embryos were injected within 30–60 min. of oviposition. Injections were made at a ~45°–60° angle and the plate was rotated to access eggs. Because eggs located in the middle of clusters were difficult to access with the micromanipulator, typically only eggs located on the perimeter were injected. Following microinjection, eggs were stored on artificial European Corn Borer Diet (Southland Products, USA) and maintained under LD 16:8 h at 25.5°C and 50% RH. After 24 h, eggs were visually checked under a dissecting microscope; those without scar tissue evidence of injection were punctured to kill (Figure S3). Approximately 7–12 eggs were typically injected per egg cluster.

Phenotyping period/pdfr injected mutants

Individuals injected with single sgRNAs targeting *period* or *pdfr* were continuously reared under LD 16:8 h at 25.5°C and 50% RH. Fourteen days after hatching, larvae were transferred into individual diet-containing 1.25 oz plastic souffle cups (WebstaurantStore) and tracked to score survivorship. Eclosion timing of wildtype, *period* and *pdfr* mutants was monitored by the Raspberry Pi-based imaging Locomotor Activity Monitor system (iLAM; Dayton & Owens, 2024), which regularly captured images at 15-min intervals. After eclosion, moths were isolated into individual mating cups and paired with two wild-type adults of the opposite sex. To score mating success, F_1 eggs were collected from each mating pair across 10 days. Both F_0 and F_1 progeny were kept for follow-up genotyping.

Phenotyping *ptth* injected mutants

Individuals injected with Cas9:dual sgRNAs targeting *ptth* or control sgRNAs were continuously reared under diapause-inducing conditions at LD 15:9 h (23.5°C). On Day 14, larvae were transferred into individual diet-containing 1.25 oz plastic souffle cups (WebstaurantStore). Individuals were weighed on day 30 and larvae who failed to pupate by day 38 were considered in diapause (Beck & Hanec, 1960; Mutchmor & Beckel, 1959).

Screening mutants

DNA was extracted in 1× DirectPCR tail lysis buffer (Viagen) containing 1 μg Proteinase K (ThermoFisher Scientific, USA) in a total volume of 100 μL. Samples were incubated for 16 h at 56°C and 85°C for 25 min. The edited region was amplified via PCR containing 1X GoTaq Master Mix (Promega), 0.2 μM target- gene-specific primers, and 1.5 uL of DNA extract in a 25 uL volume. Genotypes were resolved by PCR-based fragment size differences (e.g., Markert et al., 2016) or Sanger sequencing. For sequencing, PCRs were cleaned with the Exo-CIP™ Rapid PCR Cleanup Kit (New England Biolabs, USA) and Sanger-sequenced by Eton Bioscience Inc. (Boston, USA). DNA sequence electropherograms (.ab1) were trimmed and aligned in Geneious Prime 2023.0.4. (https://www.geneious.com). sgRNA:Cas9-generated indels were inferred by Synthego Inference of CRISPR Edits Analysis (ICE 2019.v3.0, Synthego Performance Analysis, 2019). F_0-injected individuals bearing >20% indel frequency were classified as somatic mutants. Germline editing success was determined by genotyping progeny.

Analyses

All statistical analyses were conducted in R (R Core Team, 2023). For eclosion phenotyping, the 8 h window of the day containing the greatest number of emergences was considered the main eclosion gate (Liu et al., 2023; Winfree, 1970). The main effects of sgRNA target and background on the probability of eclosing within this 8 h gate were quantified by a binomial logistic regression. Differences in the distribution of adult eclosion were compared using Watson's U^2 test within the *circular* package (Agostinelli & Lund, 2023). To evaluate evidence for epistasis between genetic background and *ptth* mutation, a linear model included the main effects of treatment (*ptth* vs. *control* sgRNA) and genetic background (Z^B vs. Z^U) on body mass. A binomial logistic regression tested these effects on diapause incidence. For all regression models, Anova() from the car package (Fox & Weisberg, 2019) determined whether the main effects of treatment,

background, and/or their interaction were significant. Significant differences between group proportions and means were respectively evaluated by Wald's Z test and Welch's t-test.

AUTHOR CONTRIBUTIONS

Jacob N. Dayton: Conceptualization; writing – original draft; writing – review and editing; supervision; investigation; methodology; formal analysis; resources; data curation. **Tammy T. Tran:** Investigation; funding acquisition; resources. **Elisa Saint-Denis:** Investigation; funding acquisition; resources; data curation. **Erik B. Dopman:** Conceptualization; funding acquisition; writing – review and editing; project administration; resources.

ACKNOWLEDGEMENTS

FUNDING INFORMATION

CONFLICT OF INTEREST STATEMENT

The authors declare no conflicts of interest.

DATA AVAILABILITY STATEMENT

All sequence and database files used in the present study are provided or cited within the text; any biological data not provided is available upon reasonable request.

ORCID

Jacob N. Dayton https://orcid.org/0000-0002-0989-8481

REFERENCES

Abdelgaffar, H., Perera, O.P. & Jurat-Fuentes, J.L. (2021) ABC transporter mutations in Cry1F-resistant fall armyworm (*Spodoptera frugiperda*) do not result in altered susceptibility to selected small molecule pesticides. *Pest Management Science*, 77(2), 949–955.

Agostinelli, C. & Lund, U. (2023) R package 'circular': Circular Statistics (version 0.5-0). Available from: https://CRAN.R-project.org/package=circular

Bassett, A.R., Tibbit, C., Ponting, C.P. & Liu, J.L. (2013) Highlight efficient targeted mutagenesis of *Drosophila* with the CRISPR/Cas9 system. *Cell Reports*, 4(1), 220–228.

Beck, S.D. & Hanec, W. (1960) Diapause in the European corn borer, Pyrausta nubilalis (Hübn.). *Journal of Insect Physiology*, 4(4), 304–318.

Brady, D., Saviane, A., Cappellozza, S. & Sandrelli, F. (2021) The circadian clock in Lepidoptera. *Frontiers in Physiology*, 12, 776826.

Coates, B.S., Dopman, E.B., Wanner, K.W. & Sappington, T.W. (2018) Genomic mechanisms of sympatric ecological and sexual divergence in a model agricultural pest, the European corn borer. *Current Opinion in Insect Science*, 26, 50–56.

Coates, B.S. & Siegfried, B.D. (2015) Linkage of an ABCC transporter to a single QTL that controls *Ostrinia nubilalis* larval resistance to the *Bacillus thuringiensis* Cry1Fa toxin. *Insect Biochemistry and Molecular Biology*, 63, 86–96.

Coates, B.S., Sumerford, D.V., Lopez, M.D., Wang, H., Fraser, L.M., Kroemer, J.A. et al. (2011) A single major QTL controls expression of larval Cry1F resistance trait in *Ostrinia nubilalis* (Lepidoptera: Crambidae) and is independent of midgut receptor genes. *Genetica*, 139(8), 961–972.

Colombani, J., Bianchini, L., Layalle, S., Pondeville, E., Dauphin-Villemant, C., Antoniewski, C. et al. (2005) Antagonistic actions of ecdysone and insulins determine final size in *Drosophila*. *Science*, 310 (5748), 667–670.

Cooper, A.M.W., Song, H., Yu, Z., Biondi, M., Bai, J., Shi, X. et al. (2021) Comparison of strategies for enhancing RNA interference efficiency in *Ostrinia nubilalis*. *Pest Management Science*, 77(2), 635–645.

Dayton, J.N. & Owens, A.C.S. (2024) iLAM: imaging locomotor activity monitor for circadian phenotyping of large-bodied flying insects. *Methods in Ecology and Evolution*, 0, 1–8.

Deem, A., Keszthelyi, A., Blackgrove, T., Vayl, A., Coffey, B., Mathur, R. et al. (2011) Break-induced replication is highly inaccurate. *PLoS Biology*, 9(2), e1000594.

DeLay, B.D., Corkins, M.E., Hanania, H.L., Salanga, M., Min Deng, J., Sudou, N. et al. (2018) Tissue-specific gene activation in *Xenopus laevis*: knockout of *lhx1* in the kidney with CRISPR/Cas9. *Genetics*, 208(2), 673–686.

Denlinger, D.L., Yocum, G.D. & Rinehart, J.P. (2012) 10—Hormonal control of diapause. In: Gilbert, L.I. (Ed.) *Insect endocrinology*. San Diego: Academic Press, pp. 430–463.

Dively, G.P., Dilip Venugopal, P., Bean, D., Whalen, J., Holmstrom, K., Kuhar, T.P. et al. (2018) Regional pest suppression associated with widespread *Bt* maize adoption benefits vegetable growers. *Proceedings of the National Academy of Sciences*, 115(13), 3320–3325.

Dopman, E.B., Bogdanowicz, S.M. & Harrison, R.G. (2004) Genetic mapping of sexual isolation between E and Z pheromone strains of the European corn borer (*Ostrinia nubilalis*). *Genetics*, 167(1), 301–309.

Dopman, E.B., Shaw, K.L., Servedio, M.R., Butlin, R.K. & Smadja, C.M. (2024) Coupling of barriers to gene exchange: causes and consequences. *Cold Spring Harbor Perspectives in Biology*, 16, 1–36. Available from: https://doi.org/10.1101/cshperspect.a041432

Farhan, Y., Smith, J.L., Sovic, M.G. & Michel, A.P. (2023) Genetic mutations linked to field-evolved Cry1Fa-resistance in the European corn borer, Ostrinia nubilalis. *Scientific Reports*, 13(1), 8081.

Fox, J. & Weisberg, S. (2019) *An R companion to applied regression*, 3rd edition. Thousand Oaks CA: Sage.

Guan, R.-B., Li, H.-C., Fan, Y.-J., Shao-Ru, H., Christiaens, O., Smagghe, G. et al. (2018) A nuclease specific to Lepidopteran insects suppresses RNAi. *The Journal of Biological Chemistry*, 293(16), 6011–6021.

Han, W.-K., Tang, F.-X., Yan, Y.-Y., Wang, Y., Zhang, Y.-X., Na, Y. et al. (2024) An OBP gene highly expressed in non-chemosensory tissues affects the phototaxis and reproduction of *Spodoptera frugiperda*. *Insect Molecular Biology*, 33(1), 81–90.

Hardin, P.E., Hall, J.C. & Rosbash, M. (1990) Feedback of the *Drosophila* period gene product on circadian cycling of its messenger RNA levels. *Nature*, 343(6258), 536–540.

Hardin, P.E., Hall, J.C. & Rosbash, M. (1992) Circadian oscillations in period gene mRNA levels are transcriptionally regulated. *Proceedings of the National Academy of Sciences*, 89(24), 11711–11715.

Hyun, S., Lee, Y., Hong, S.-T., Bang, S., Paik, D., Kang, J. et al. (2005) *Drosophila* GPCR Han is a receptor for the circadian clock neuropeptide PDF. *Neuron*, 48(2), 267–278.

Ikeda, K., Daimon, T., Shiomi, K., Udaka, H. & Numata, H. (2021) Involvement of the clock gene period in the photoperiodism of the Silkmoth *Bombyx mori*. *Zoological Science*, 38(6), 523–530.

Ikten, C., Skoda, S.R., Hunt, T.E., Molina-Ochoa, J. & Foster, J.E. (2011) Genetic variation and inheritance of diapause induction in two

distinct voltine ecotypes of *Ostrinia nubilalis* (Lepidoptera: Crambidae). *Annals of the Entomological Society of America*, 104(3), 567–575.

Khajuria, C., Buschman, L.L., Chen, M.S., Siegfried, B.D. & Zhu, K.Y. (2011) Identification of a novel aminopeptidase P-like gene (OnAPP) possibly invovled in Bt toxicity and resistance in a major corn pest (*Ostrinia nubilalis*). *PLoS One*, 6(8), e23983.

Konopka, R.J. & Benzer, S. (1971) Clock mutants of *Drosophila* melanogaster. *Proceedings of the National Academy of Sciences of the United States of America*, 68(9), 2112–2116.

Kozak, G.M., Wadsworth, C.B., Kahne, S.C., Bogdanowicz, S.M., Harrison, R.G., Coates, B.S. et al. (2019) Genomic basis of circannual rhythm in the European corn borer moth. *Current Biology*, 29(20), 3501–3509.e5.

Kroll, F., Powell, G.T., Ghosh, M., Gestri, G., Antinucci, P., Hearn, T.J. et al. (2021) A simple and effective F0 knockout method for rapid screening of behaviour and other complex phenotypes. *eLife*, 10, 1–34. Available from: https://doi.org/10.7554/eLife.59683

Lassance, J.-M., Groot, A.T., Liénard, M.A., Antony, B., Borgwardt, C., Andersson, F. et al. (2010) Allelic variation in a fatty-acyl reductase gene causes divergence in moth sex pheromones. *Nature*, 466(7305), 486–489.

Lear, B.C., Elaine Merrill, C., Lin, J.-M., Schroeder, A., Zhang, L. & Allada, R. (2005) A G protein-coupled receptor, groom-of-PDF, is required for PDF neuron action in circadian behavior. *Neuron*, 48(2), 221–227.

Levy, R.C., Kozak, G.M., Wadsworth, C.B., Coates, B.S. & Dopman, E.B. (2015) Explaining the sawtooth: latitudinal periodicity in a circadian gene correlates with shifts in generation number. *Journal of Evolutionary Biology*, 28(1), 40–53.

Li, J.-J., Shi, Y., Ji-Nan, W., Li, H., Smagghe, G. & Liu, T.-X. (2021) CRISPR/Cas9 in Lepidopteran insects: progress, application and prospects. *Journal of Insect Physiology*, 135(October), 104325.

Lin, Y., Stormo, G.D. & Taghert, P.H. (2004) The neuropeptide pigment-dispersing factor coordinates pacemaker interactions in the *Drosophila* circadian system. *The Journal of Neuroscience*, 24(36), 7951–7957.

Liu, X., Cai, L., Zhu, L., Tian, Z., Shen, Z., Cheng, J. et al. (2023) Mutation of the clock gene timeless disturbs diapause induction and adult emergence rhythm in *Helicoverpa armigera*. *Pest Management Science*, 79(5), 1876–1884.

Mackay, T.F.C. & Anholt, R.R.H. (2024) Pleiotropy, epistasis and the genetic architecture of quantitative traits. *Nature Reviews Genetics*, 25, 639–657. Available from: https://doi.org/10.1038/s41576-024-00711-3

Markert, M.J., Zhang, Y., Enuameh, M.S., Reppert, S.M., Wolfe, S.A. & Merlin, C. (2016) Genomic access to monarch migration using TALEN and CRISPR/Cas9-mediated targeted mutagenesis. *G3: Genes, Genomes, Genetics*, 6(4), 905–915.

McBrayer, Z., Ono, H., Shimell, M., Parvy, J.-P., Beckstead, R.B., Warren, J.T. et al. (2007) Prothoracicotropic hormone regulates developmental timing and body size in *Drosophila*. *Developmental Cell*, 13(6), 857–871.

Mertens, I., Vandingenen, A., Johnson, E.C., Shafer, O.T., Li, W., Trigg, J.S. et al. (2005) PDF receptor signaling in *Drosophila* contributes to both circadian and geotactic behaviors. *Neuron*, 48(2), 213–219.

Mutchmor, J.A. & Beckel, W.E. (1959) Some factors affecting diapause in the European corn borer, *Ostrinia nubilalis* (Hbn.) (Lepidoptera: Pyralidae). *Canadian Journal of Zoology*, 37, 161–168.

Myers, E.M., Jiujiu, Y. & Sehgal, A. (2003) Circadian control of Eclosion: interaction between a central and peripheral clock in *Drosophila* melanogaster. *Current Biology*, 13(6), 526–533.

Nambiar, T.S., Baudrier, L., Billon, P. & Ciccia, A. (2022) CRISPR-based genome editing through the lens of DNA repair. *Molecular Cell*, 82(2), 348–388.

Nartey, M.A., Sun, X., Qin, S., Hou, C.-X. & Li, M.-W. (2021) CRISPR/Cas9-based knockout reveals that the clock gene timeless is

indispensable for regulating circadian behavioral rhythms in *Bombyx mori*. *Insect Science*, 28(5), 1414–1425.

NC. (2024) NC246: ecology and management of arthropods in corn. Available from: https://nimss.org/projects/view/mrp/outline/18695

Peng, Y., Stoleru, D., Levine, J.D., Hall, J.C. & Rosbash, M. (2003) *Drosophila* free-running rhythms require intercellular communication. *PLoS Biology*, 1(1), E13.

Perera, O.P., Little, N.S. & Pierce, C.A., III. (2018) CRISPR/Cas9 mediated high efficiency knockout of the eye color gene Vermillion in Helicoverpa zea (Boddie). *PLoS One*, 13(5), e0197567.

Pezzini, D., Taylor, K.L., Reisig, D.D. & Fritz, M.L. (2024) Cross-pollination in seed-blended refuge and selection for Vip3A resistance in a Lepidopteran pest as detected by genomic monitoring. *Proceedings of the National Academy of Sciences*, 121(13), e2319838121.

Qiu, J. & Hardin, P.E. (1996) Developmental state and the circadian clock interact to influence the timing of eclosion in *Drosophila* melanogaster. *Journal of Biological Rhythms*, 11(1), 75–86.

R Core Team. (2023) R: a language and environment for statistical computing. R Foundation for Statistical Computing. Available from: https://www.R-project.org/

Renn, S.C., Park, J.H., Rosbash, M., Hall, J.C. & Taghert, P.H. (1999) A PDF neuropeptide gene mutation and ablation of PDF neurons each cause severe abnormalities of behavioral circadian rhythms in *Drosophila*. *Cell*, 99(7), 791–802.

Rewitz, K.F., Yamanaka, N., Gilbert, L.I. & O'Connor, M.B. (2009) The insect neuropeptide PTTH activates receptor tyrosine kinase torso to initiate metamorphosis. *Science*, 326(5958), 1403–1405.

Ruf, F., Mitesser, O., Mungwa, S.T., Horn, M., Rieger, D., Hovestadt, T. et al. (2021) Natural zeitgebers under temperate conditions cannot compensate for the loss of a functional circadian clock in timing of a vital behavior in *Drosophila*. *Journal of Biological Rhythms*, 36(3), 271–285.

Sakurai, S. (1983) Temporal organization of endocrine events underlying larval-larval ecdysis in the silkworm, *Bombyx mori*. *Journal of Insect Physiology*, 29(12), 919–932.

Selcho, M., Millán, C., Palacios-Muñoz, A., Ruf, F., Ubillo, L., Chen, J. et al. (2017) Central and peripheral clocks are coupled by a neuropeptide pathway in *Drosophila*. *Nature Communications*, 8(May), 15563.

Shimell, M., Pan, X., Martin, F.A., Ghosh, A.C., Leopold, P., O'Connor, M.B. et al. (2018) Prothoracicotropic hormone modulates environmental adaptive plasticity through the control of developmental timing. *Development*, 145(6), 1–13. Available from: https://doi.org/10.1242/dev.159699

Smith, J.L., Farhan, Y. & Schaafsma, A.W. (2019) Practical resistance of *Ostrinia nubilalis* (Lepidoptera: Crambidae) to Cry1F *Bacillus thuringiensis* maize discovered in Nova Scotia, Canada. *Scientific Reports*, 9(1), 1–10.

Smith, W. & Rybczynski, R. (2012) 1—Prothoracicotropic hormone. In: Gilbert, L.I. (Ed.) *Insect endocrinology*. San Diego: Academic Press, pp. 1–62.

Synthego Performance Analysis. (2019) ICE analysis. v3.0. Synthego.

Taning, C.N., van Tizi, B., Eynde, N.Y., Ma, S. & Smagghe, G. (2017) CRISPR/Cas9 in insects: applications, best practices and biosafety concerns. *Journal of Insect Physiology*, 98(April), 245–257.

Terenius, O., Papanicolaou, A., Garbutt, J.S., Eleftherianos, I., Huvenne, H., Kanginakudru, S. et al. (2011) RNA interference in Lepidoptera: an overview of successful and unsuccessful studies and implications for experimental design. *Journal of Insect Physiology*, 57(2), 231–245.

Tigano, A. & Friesen, V.L. (2016) Genomics of local adaptation with gene flow. *Molecular Ecology*, 25(10), 2144–2164.

Truman, J.W. (1972) Physiology of insect rhythms: II. The silkmoth brain as the location of the biological clock controlling eclosion. *Journal of Comparative Physiology*, 81, 99–114. Available from: https://doi.org/10.1007/BF00693553

Truman, J.W. & Riddiford, L.M. (1974) Physiology of insect rhythms: III. The temporal organization of the endocrine events underlying pupation of the tobacco hornworm. *The Journal of Experimental Biology*, 60(2), 371–382.

Turner, T.L. (2014) Fine-mapping natural alleles: quantitative complementation to the rescue. *Molecular Ecology*, 23(10), 2377–2382.

Uchibori-Asano, M., Kayukawa, T., Sezutsu, H., Shinoda, T. & Daimon, T. (2017) Severe developmental timing defects in the prothoracicotropic hormone (PTTH)-deficient silkworm, *Bombyx mori*. *Insect Biochemistry and Molecular Biology*, 87(August), 14–25.

Unbehend, M., Kozak, G.M., Koutroumpa, F., Coates, B.S., Dekker, T., Groot, A.T. et al. (2021) bric à brac controls sex pheromone choice by male European corn borer moths. *Nature Communications*, 12(1), 2818.

Vaze, K.M. & Helfrich-Förster, C. (2021) The neuropeptide PDF is crucial for delaying the phase of *Drosophila's* evening neurons under long zeitgeber periods. *Journal of Biological Rhythms*, 36(5), 442–460.

Winfree, A.T. (1970) Integrated view of resetting a circadian clock. *Journal of Theoretical Biology*, 28(3), 327–374.

Yoshii, T., Wülbeck, C., Sehadova, H., Veleri, S., Bichler, D., Stanewsky, R. et al. (2009) The neuropeptide pigment-dispersing factor adjusts period and phase of *Drosophila*'s clock. *The Journal of Neuroscience*, 29(8), 2597–2610.

Yu, Y. (2022) Genetic basis of seasonal timing in two moth species. PhD dissertation, Tufts University.

Wang, Y., Li, Z., Xu, J., Zeng, B., Ling, L., You, L. et al. (2013) The CRISPR/-Cas system mediates efficient genome engineering in *Bombyx mori*. *Cell Research*, 23(12), 1414–1416.

Wu, R.S., Lam, I.I., Clay, H., Duong, D.N., Deo, R.C. & Coughlin, S.R. (2018) A rapid method for directed gene knockout for screening in G0 zebrafish. *Developmental Cell*, 46, 112–125.

Zhang, Z.-J., Liu, X.-J., Ye, Y., Yang, F.-Y. & Li, K. (2021) The receptor tyrosine kinase torso regulates ecdysone homeostasis to control developmental timing in *Bombyx mori*. *Insect Science*, 28(6), 1582–1590.

Zhao, J., Tan, Y., Jiang, Y., Zhu-Salzman, K. & Xiao, L. (2023) CRISPR/Cas9-mediated methoprene-tolerant 1 knockout results in precocious metamorphosis of beet armyworm (*Spodoptera Exigua*) only at the late larval stage. *Insect Molecular Biology*, 32(2), 132–142.

Zhu, G.-H., Chereddy, S.C.R.R., Howell, J.L. & Palli, S.R. (2020) Genome editing in the fall armyworm, *Spodoptera frugiperda*: multiple SgRNA/Cas9 method for identification of knockouts in one generation. *Insect Biochemistry and Molecular Biology*, 122(July), 103373.

SUPPORTING INFORMATION

Additional supporting information can be found online in the Supporting Information section at the end of this article.

Data S1. Supporting Information.

Table S1. Oligos designed for sgRNA templates and primer pairs to detect mutations at *period*, *pdf receptor-like* (*pdfr*), and *prothoracicotropic hormone* (*ptth*) genes in *Ostrinia nubilalis*. The bolded sequences denote the sgRNA target in the *Ostrinia nubilalis* genome.

Figure S1. *period* but not *pdfr* mutagenesis reduces rhythmic strength in wildtype eclosion timing.

Figure S2. *period* but not *pdfr* mutagenesis disrupts normal eclosion timing.

Figure S3. Microinjection of *Ostrinia nubilalis* embryos.

> **How to cite this article:** Dayton, J.N., Tran, T.T., Saint-Denis, E. & Dopman, E.B. (2024) Efficient CRISPR/Cas9-mediated genome editing in the European corn borer, *Ostrinia nubilalis*. *Insect Molecular Biology*, 1–11. Available from: https://doi.org/10.1111/imb.12959